JOURNAL OF SOLID STATE CHEMISTRY 51, 376–387 (1984)

Synthesis, Crystal Structure, and Magnetism of $FeMoO_4Cl$, a New Two-Dimensional Antiferromagnet with O—Mo—O Superexchange Pathways

C. C. TORARDI[1] AND J. C. CALABRESE

Central Research and Development Department,[2] E. I. Du Pont de Nemours and Company, Experimental Station, Wilmington, Delaware 19898

AND K. LÁZÁR[3] AND W. M. REIFF[1]

Department of Chemistry, Northeastern University, Boston, Massachusetts 02115

Received August 3, 1983; in revised form October 20, 1983

$FeMoO_4Cl$ crystallizes in the tetragonal system with unit cell dimensions $a = 6.672(3)$ and $c = 5.223(3)$ Å in space group $P4/nmm$ with $Z = 2$. The structure is built from $FeMoO_4Cl$ layers stacked along the c axis and is closely related to α-$VOPO_4$-type compounds. Individual layers can be described as sheets of corner-sharing MoO_4 tetrahedra and FeO_4Cl square pyramids. The temperature dependence of χ'_M for a powder sample exhibits a broad maximum at 104 K characteristic of extensive short range antiferromagnetic correlation within the layers. This is a result of surprisingly strong Fe(III)–Fe(III) exchange interactions transmitted by O—Mo—O pathways. Long range three-dimensional order is confirmed by the hyperfine splitting of the zero field Mössbauer spectrum, $T_{Néel} = 69.2 \pm 0.1$ K. Analysis of the combined quadrupole-Zeeman split hyperfine spectrum of the powder at 1.7 K leads to $\theta = 90°$ for the angle between the internal hyperfine field (H_{hf}) and V_{zz}, the principal axis of the electric field gradient. Single crystal Mössbauer and X-ray powder diffraction data are also discussed.

Introduction

A recent study of the system LnOCl: MoO_3 (Ln = La through Tm, and Y) found two different structures with composition $LnMoO_4Cl$ (*1, 2*). A structural transition occurs when the size of the trivalent cation is equal to or smaller than Sm^{3+}. An entirely different atomic arrangement was predicted for the compound $FeMoO_4Cl$ due to the very small size of the ferric ion. The structure of this new tetragonal phase, reported here, consists of layers containing square pyramidal Fe^{3+} and tetrahedral Mo^{6+}. Structurally, it is closely related to the layered materials $NbOPO_4$ (*3*), $VOMoO_4$ (*4*), $MoOPO_4$ (*5*), and α-$VOPO_4$ (*6*). As a consequence of its sheet-like structure, the new compound exhibits low dimensional magnetic interactions.

In recent years, there have been a number of studies of magnetically two-dimen-

[1] To whom correspondence should be addressed.

[2] Contribution No. 3316.

[3] On leave from the Institute of Isotopes, Hungarian Academy of Sciences, Budapest, Hungary.

0022-4596/84 $3.00

sional (2D) materials. These include both ferromagnetic and antiferromagnetic layer materials such as $(RNH_3)_2CuCl_4$ (*7*) and $(RNH_3)_2MCl_4$ (M = Fe (*8*), Mn (*9*)), respectively. Within the latter series of antiferromagnets, the susceptibility maximum for the iron system is relatively sharp indicating the absence of extensive short-range order above the observed susceptibility anomaly. On the other hand, $[CH_3NH_3]_2MnCl_4$, and another entire group of systems, typified by compounds such as K_2MnF_4 (*10*), Rb_2MnF_4 (*11*), Rb_2FeF_4 (*12*), K_2NiF_4 (*13*), and K_2CoF_4 (*13*) exhibit broad susceptibility maxima ($T_{\chi max}$) suggesting considerable short range antiferromagnetic correlation for temperatures well above any cooperative long range (3D) ordering temperature. The most readily apparent common feature for all of the preceding is that they contain divalent transition metal ions whose intralayer superexchange involves single atom (halogen) bridges. In the present work, we also report on the magnetic properties of a trivalent iron system for which rather long O—Mo—O bridging units result in surprisingly strong intralayer superexchange and 2D magnetic behavior.

Experimental

Synthesis

MoO_3 (Fisher Certified A.C.S.), Fe_2O_3 (Alfa, 99.9%), and $FeCl_3$ (Alfa, 98%) were ground together in a 3 : 1 : 1.05 molar ratio under an inert atmosphere and sealed in an evacuated glass ampoule. The tube was heated at 360°C for 18 hr and allowed to cool. The resulting dark-red crystalline platelets were washed in air with acetone to remove unreacted $FeCl_3$ and then air-dried. A crystalline product could also be obtained at reaction temperatures as low as 300°C, or by reacting FeOCl (made from $FeCl_3$ and Fe_2O_3) and MoO_3 in an equimolar ratio at 400°C. X-ray powder diffraction patterns of individual $FeMoO_4Cl$ preparations often showed a small amount of MoO_3, FeOCl, or Fe_2O_3 as an impurity. A pure phase was obtained by reacting $Fe_2(MoO_4)_3$ (prepared as described in the literature (*14*)) with excess $FeCl_3$ in an evacuated glass tube at 350°C, and by washing the product with acetone. Chemical composition was established from single crystal X-ray diffraction data as well as from chemical analyses on powdered crystals. Calculated for $FeMoO_4Cl$: Mo, 38.2; Fe, 22.2; Cl, 14.1. Found: Mo, 38.6; Fe, 22.5; Cl, 13.4. When in pure and powdered form, $FeMoO_4Cl$ is yellow–green. It appears stable in air to 200°C but is slowly decomposed in cold water.

X-Ray Powder Diffraction

A Guinier-Hägg focusing camera (r = 40 mm) was used to obtain X-ray powder diffraction data. The radiation was monochromatic Cu$K_{\alpha 1}$ (λ = 1.5405 Å). Silicon powder (a = 5.4305 Å) was used as an internal standard. Line positions on the film were determined to ±5 μm with a David Mann film reader (a precision screw, split-image comparator). Intensities were estimated by oscilloscopic comparison of film density with the strongest line of the pattern. Lattice parameters for $FeMoO_4Cl$ were calculated by a least squares refinement of the Guinier data. The indexed X-ray powder diffraction pattern recorded at room temperature is given in Table I. It was indexed as tetragonal with a = 6.6694(4) and c = 5.228(1) Å.

Single Crystal X-Ray Structure Determination

A single crystal of $FeMoO_4Cl$ was obtained from the sealed-tube reaction product. The crystal, a flat plate with dimensions 0.14 × 0.30 × 0.32 mm was placed on an Enraf-Nonius CAD4 X-ray diffractometer equipped with monochromatic MoK_α ra-

TABLE I

X-RAY POWDER DIFFRACTION DATA FOR $FeMoO_4Cl$[a,b]

2θ(obs)	I(obs)	I(calc)	hkl	d(obs)	d(calc)
16.960	50	44	001	5.223	5.228
21.579	40	21	101	4.115	4.115
25.427	90	95	111	3.500	3.502
26.724	100	100	200	3.333	3.335
31.806	45	21	201	2.811	2.811
38.144	45	17	220	2.357	2.358
39.370	60	49	112	2.287	2.286
41.988	15	6	221	2.150	2.149
44.231	15	6	301	2.046	2.046
46.381	60	26	311	1.956	1.956
		26	131		1.956
55.036	50	13	400	1.667	1.667
55.978	70	35	312	1.641	1.641
		35	132		1.641
57.997	5	4	401	1.589	1.589
59.789	10	2	411	1.545	1.545
		2	141		1.545
		9	203		1.544
61.527	5	4	331	1.506	1.505
62.195	40	11	420	1.491	1.491
		11	240		1.491
64.972	5	5	421	1.434	1.434
		5	241		1.434
66.632	5	9	223	1.402	1.401
69.727	5	8	332	1.347	1.347
72.191	2	1	510	1.307	1.308
		1	150		1.308
		1	004		1.307
73.163	2	1	341	1.292	1.292
		1	431		1.292
74.745	5	5	511	1.269	1.269
		5	151		1.269
81.578	2	4	440	1.179	1.179
82.311	5	5	512	1.170	1.170
		5	152		1.170
86.902	2	<1	522	1.120	1.120

[a] Tetragonal with $a = 6.6694(4)$ and $c = 5.228(1)$ Å.
[b] $F_{20} = 42(0.011, 42)$; $M_{20} = 54$.

diation. After careful crystal alignment, 25 diffraction maxima were located and used to obtain cell parameters and orientation matrix. The reflections indexed in a tetragonal cell with dimensions $a = 6.672(3)$ and $c = 5.223(3)$ Å. For $Z = 2$, the calculated density is 3.59 g/cm^3.

A total of 927 reflections were collected by the θ-2θ mode from $3 \leq \theta \leq 35°$ and merged to yield 304 independent data with $I \geq 2\sigma(I)$ in 4/*mmm* symmetry. The data were treated in the usual fashion for Lorentz and polarization effects with $P = 0.055$. An analytical correction for absorption was also applied using a Gaussian grid of $8 \times 8 \times 8$. The crystal faces and distances (millimeters) from the center were ± [$\bar{1}11$, 0.110; $11\bar{1}$, 0.186; $1\bar{1}1$, 0.110; 111, 0.159; $\bar{1}01$, 0.146; 101, 0.098; 012, 0.098; $01\bar{2}$, 0.061; 001, 0.073]. The transmission factors for the crystal ($\mu = 62.3$ cm^{-1}) varied from 0.25 to 0.57. There was no evidence of radiation damage during the data collection.

An examination of the data revealed systematic absences compatible with space group *P4/nmm* (No. 129). The structure was determined using the heavy atom method, and all atoms were located on mirror planes. Full matrix least-squares refinement on all positional and anisotropic thermal parameters including terms for anomalous dispersion for Mo, Fe, and Cl and for anisotropic extinction converged with $R = 0.024$ and $R_w = 0.033$. The largest peak in a final difference Fourier was 0.78 e/Å^3 near the molybdenum atom.

Atomic positional and thermal parameters for $FeMoO_4Cl$ are listed in Table II. Important interatomic distances and angles are given in Table III, and atomic labels correspond to those in Figs. 1 and 3.[4]

Magnetic Susceptibility Measurements and Mössbauer Spectroscopy

The magnetic susceptibility and zero field Mössbauer spectra were determined using apparatus previously described (*15*).

[4] All crystallographic calculations were performed on a Digital Equipment Corp. VAX 11/780 computer using a system of programs developed by J. C. Calabrese. Structural plots were made with the ORTEP program (C. K. Johnson, 1971).

TABLE II

POSITIONAL AND THERMAL[a] PARAMETERS FOR THE ATOMS OF $FeMoO_4Cl$[b]

Atom	x	y	z	U_{11}	U_{22}	U_{33}	U_{12}	U_{13}	U_{23}
Mo	0.75	0.25	0.00	7.4(2)	7.4	16.7(2)	0	0	0
Fe	0.75	0.75	0.7272(1)	8.7(2)	8.7	12.1(2)	0	0	0
Cl	0.75	0.75	0.3044(2)	38.0(4)	38.0	13.4(4)	0	0	0
O	0.75	0.0367(2)	0.8032(3)	27.3(6)	9.9(5)	25.0(6)	0	0	−3.6(5)

[a] (×1000).
[b] Space group *P4/nmm* (No. 129).

Results and Discussion

Structure Description

The crystal structure of $FeMoO_4Cl$ is very similar to that of α-$VOPO_4$ (*6*) with iron and chlorine replacing the vanadyl group, and molybdate replacing phosphate. From one view, the structure of $FeMoO_4Cl$ may be pictured as consisting of chains of corner-shared FeO_4Cl_2 octahedra, linked via *trans* Cl atoms, and extended along the *c* axis. These chains are interconnected by MoO_4 tetrahedra such that every FeO_4Cl_2 octahedron shares its four equatorial oxygen corners with four molybdate tetrahedra. However, the iron atoms within the octahedra are shifted toward one chlorine atom and away from the other (i.e., FeO_4ClCl' octahedra). This disruption in the bonding forces along the *c* axis makes a structural description based on two-dimensional layers especially suitable and, as will be seen subsequently, is most consistent with the combined susceptibility and Mössbauer results.

In the alternative view, the structure may be described as consisting of $FeMoO_4Cl$ layers stacked along the *c* axis. These layers contain four-coordinated molybdenum(VI) and five-coordinated iron(III). A portion of two stacked layers showing the essential atomic arrangement is given in Fig. 1. All atoms in this structure lie on one or more mirror planes. Molybdenum is bound to four oxygen atoms in a slightly distorted tetrahedral arrangement with $\bar{4}2m$ (D_{2d}) site symmetry. Because all oxygen atoms in this structure are crystallographi-

TABLE III

IMPORTANT INTERATOMIC DISTANCES AND ANGLES IN $FeMoO_4Cl$

	Intralayer distances (Å)		
Fe—Cl	2.209(2)	Oa—Ob	2.705(2)
Fe—Oa	1.954(1)	Oa—Oe	2.846(3)
Mo—Oa	1.756(1)	Oa—Of	2.877(3)
Oa—Cl	3.232(2)		
	Interlayer distances (Å)		
Fe—Cl	3.015(2)	Oa—Cl	3.243(2)
	Angles (deg)		
Cl—Fe—Oa	101.7(1)	Fe—Oa—Mo	155.9(1)
Oa—Fe—Ob	87.6(1)	Oa—Mo—Oe	108.3(1)
Oa—Fe—Oc	156.6(1)	Oa—Mo—Of	110.1(1)

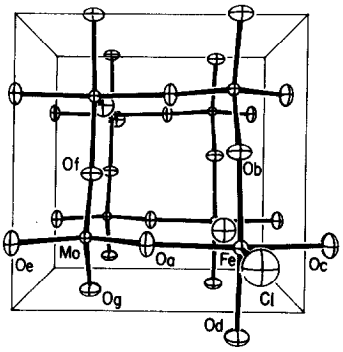

FIG. 1. A view down the *c* axis of $FeMoO_4Cl$ showing the atomic arrangement of two stacked layers.

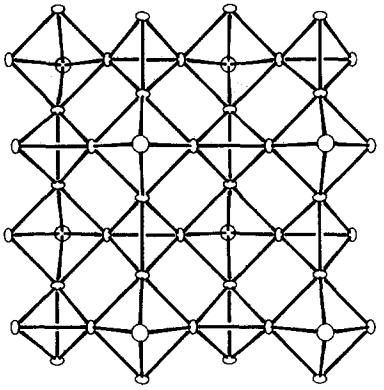

FIG. 2. A section of an $FeMoO_4Cl$ layer represented by corner-sharing MoO_4 tetrahedra and FeO_4Cl square pyramids (metal atoms not shown).

cally equivalent, the distortion from true tetrahedral symmetry is seen only in the O—Mo—O bond angles of 108.3° and 110.1° (109.5° average). The molybdenum–oxygen bond length of 1.756(1) Å compares well with the sum of ionic radii for Mo^{6+} and O^{2-}, 1.76 Å (*16*). Iron is bonded to four oxygen atoms at 1.954(1) Å and one chlorine atom at 2.209(2) Å in a square pyramidal fashion, site symmetry *4mm* (C_{4v}), with chlorine at the apex. The iron atom is located 0.4 Å above the plane of the four basal oxygen atoms. A similar atomic arrangement has been observed in the molecular square pyramidal complexes $Fe(S_2CN(C_2H_5)_2)_2Cl$ (*17*) and $Fe(CH_3COCHCOCH_3)_2Cl$ (commonly named $Fe(acac)_2Cl$) (*18*). In the latter compound, the iron–oxygen and iron–chlorine distances of 1.95 and 2.213 Å, respectively, compare well with those in the new compound. Within the $FeMoO_4Cl$ layers, each of the four oxygen atoms bonded to molybdenum is shared with an iron atom and vice versa. Thus, the layer composition can be represented as $FeClO_{4/2}MoO_{4/2}$.

Alternatively, the layer can be described as a two-dimensional sheet composed of corner-sharing tetrahedra and square pyramids. Figure 2 shows a section of an $FeMoO_4Cl$ layer with each MoO_4 tetrahedron sharing its four corners with the basal corners of four separate FeO_4Cl square pyramids. The pyramids alternate with their apices (i.e., chlorine atoms) pointing above and below the layer. The shortest chlorine–chlorine distance on one side of a layer is 6.67 Å which is the unit-cell repeat distance.

Layers stack directly above one another with the vertices of one layer fitting into the hollows of the next layer. Because the chlorine atom nets are very open, adjacent layers interpenetrate one another. Each chlorine atom nestles into the pocket formed by the four basal FeO_4Cl oxygen atoms of a neighboring layer. This results in alternating short and long Fe—Cl distances along the *c* axis of 2.209(2) and 3.015(2) Å, respectively. The latter distance can be assigned to a weak Fe—Cl interaction with an estimated bond order of 0.1 (*19*). Cohesion between layers results from these weak interlayer Fe—Cl bonds as well as induced dipole–dipole interactions. A section of two stacked layers viewed perpendicular to the c axis is shown in Fig. 3. The shortest Cl—Cl distance of 5.14 Å involves atoms from adjacent layers.

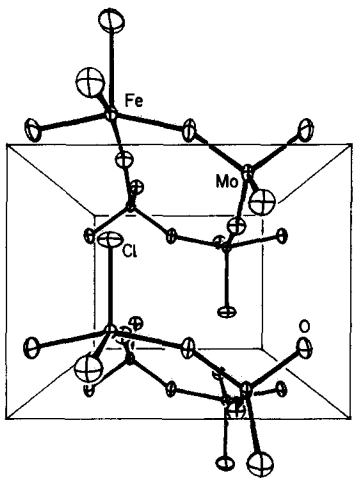

FIG. 3. A view perpendicular to the *c* axis (vertical) of $FeMoO_4Cl$ showing two stacked layers.

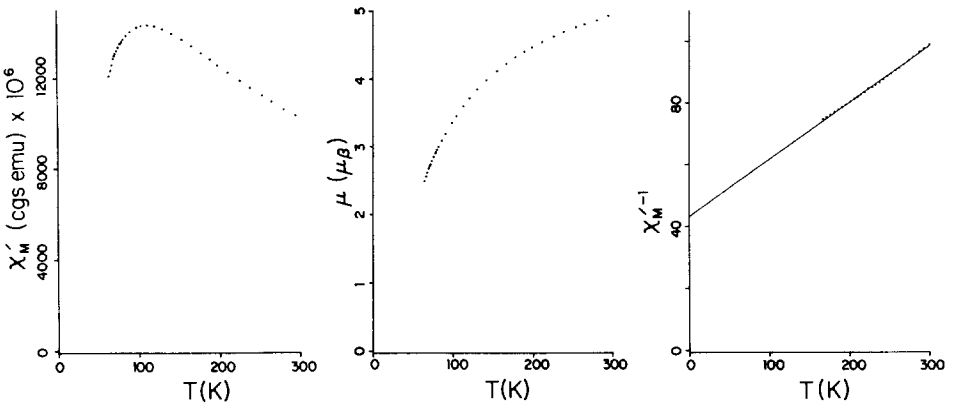

FIG. 4. The temperature dependence of the corrected molar susceptibility (left), magnetic moment (center), and reciprocal susceptibility (right) for $FeMoO_4Cl$, H_0 = 5.1 kG.

Thus far, chemical variations of Fe MoO_4Cl appear to be limited. Attempts to substitute iron with scandium, chromium, or manganese, molybdenum with tungsten or chromium, and chlorine with bromine have been unsuccessful. Presently, the intercalation chemistry of $FeMoO_4Cl$ is under investigation, and the compounds M_xFe MoO_4Cl containing reduced iron have been successfully prepared with M = Li or Na and $x \simeq 1$ (*20*).

Magnetic Susceptibility and ESR

The temperature dependence of the corrected molar susceptibility (χ'_M) and magnetic moment (μ) over the range 300 to 50 K are shown in Fig. 4, while sample moment data are given in Table IV. There is no evidence of field dependence for H_0 varying from 1.6 to 5.1 kG in this temperature range. At ambient temperature, μ is already well below the expected spin only value (5.92 μ_β) for high-spin iron(III). This fact and the steady decrease in μ with temperature clearly indicate strong antiferromagnetic exchange. Note that the molybdenum is hexavalent (d^0) and as such is diamagnetic and cannot contribute to the paramagnetism of the compound. Examination of χ'_M vs T shows a broad maximum centered at ~105 K and in view of the layer structure suggests two-dimensional antiferromagnetism. The result of least squares computer fits to $\chi'^{-1}_M = T - \theta/C$ for 10 magnetic fields is a Curie–Weiss law whose parameters are: the paramagnetic Curie temperature $\theta = -207$ K, $\mu_{eff} = 6.30$, and C = 4.96 emu/mole. The reciprocal susceptibility deviates from this law for $T \leq \sim 190$ K, i.e., well above $T_{\chi max}$ (105 K) (Fig. 4). This is consistent with *extensive* short range intralayer AF correlation. Exchange is evident in the ESR spectrum at ambient temperature (Fig. 5). For the local ferric ion symmetry C_{4v} *axial*, one would normally expect well-defined resonances at $g_{effective}$ = 2 and 6. The observed spectrum is a broad, rather featureless trace centered at $g \sim 2$

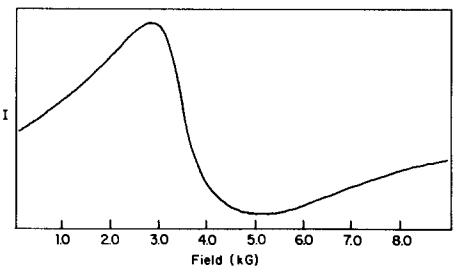

FIG. 5. X-Band ESR spectrum of $FeMoO_4Cl$ at ambient temperature.

TABLE IV

SAMPLE MAGNETIC MOMENT DATA FOR $FeMoO_4Cl$

Temperature (K)	Magnetic moment (Bohr magneton)
296.00	4.96
281.61	4.90
266.09	4.84
254.72	4.79
239.61	4.72
226.77	4.65
211.81	4.56
199.31	4.48
189.72	4.42
178.69	4.34
167.13	4.24
155.15	4.13
142.17	3.99
130.68	3.85
121.04	3.73
112.81	3.60
104.16	3.46
98.87	3.36
90.53	3.19
85.72	3.09
82.00	3.00
80.14	2.96
78.63	2.92
77.65	2.90
75.75	2.85
73.55	2.79
71.70	2.74
70.78	2.72
69.55	2.68
67.92	2.62
66.32	2.56
66.19	2.49

and typical of exchange broadening effects. The value of J, the intralayer exchange parameter, can be estimated from $T_{\chi max}$ using the relation $KT_{\chi max}/JS(S + 1) = 2.05$ for a quadratic Heisenberg 2D planar magnet (*21*). Using this expression, one finds $|J| = 4.1\ cm^{-1}$ ($J/k_B = 5.8$ K). This is to be compared to values of 4.1 and 3.3 K determined for K_2MnF_4 and Rb_2MnF_4, respectively (*10, 11*), two-dimensional d^5 systems. Additional low temperature magnetic susceptibility measurements to 1.75 K show that

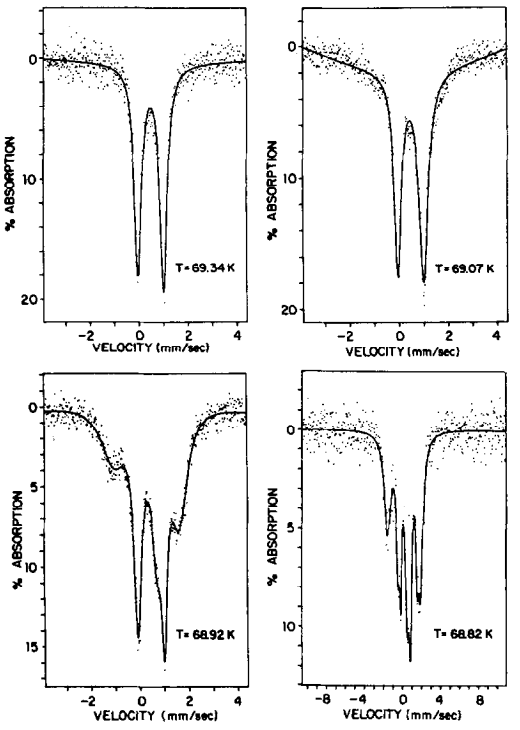

FIG. 6. Zero field Mössbauer spectra of $FeMoO_4Cl$ in the temperature range 69.34 to 68.82 K.

the magnetic moment steadily continues to decrease, $\mu = 0.47\ \mu_B$ at 1.75 K. However, there are no obvious additional magnetic phase transformations. In fact, χ'_M starts to gradually increase below ~30 K, reflecting what we believe to be the effects of trace (perhaps Curie–Weiss law) impurities.

Zero Field Mössbauer Spectra

The cooperative three-dimensional ordering expected for some temperature $T_{Néel} < T_{\chi max}$ is clearly evident in the temperature dependence of the zero field Mössbauer spectra, (Figs. 6 and 7) as discussed subsequently. At ambient temperature a single, nearly symmetric quadrupole doublet is observed. The observed isomer shift (δ) for the five-coordinate FeO_4Cl chromophore (Table V) nicely fits the expected systematics of δ with coordination number, i.e., δ increasing with increasing coordina-

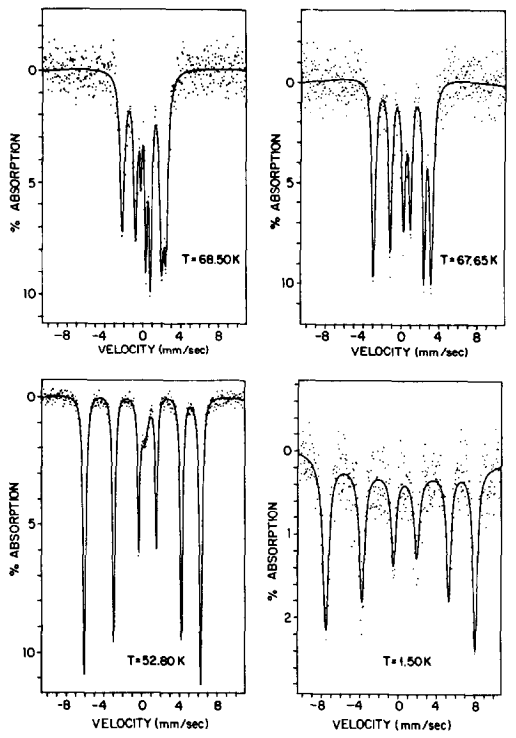

FIG. 7. Zero field Mössbauer spectra of $FeMoO_4Cl$ in the temperature range 68.50 to 1.50 K.

TABLE V

MÖSSBAUER PARAMETERS[a] FOR $FeMoO_4Cl$ ABOVE $T_{Néel}$

T (K)	δ	ΔE	Γ
	(mm sec^{-1})		
70.0	0.354	1.041	0.366
70.5	0.356	1.040	0.371
71.24	0.355	1.038	0.352
72.23	0.355	1.038	0.349
73.91	0.356	1.032	0.349
76.05	0.356	1.030	0.344
79.9	0.354	1.024	0.338
83.0	0.354	1.019	0.346
92.7	0.355	1.006	0.348
102.3	0.356	0.998	0.345
112.95	0.358	0.986	0.350
122.68	0.357	0.976	0.347
133.7	0.357	0.967	0.347
147.9	0.356	0.952	0.347
160.25	0.358	0.943	0.358
173.4	0.358	0.936	0.364
191.5	0.355	0.924	0.341
220.9	0.356	0.912	0.354
300.0	0.357	0.889	0.306

[a] Relative to natural iron, source and absorber always at the same temperature.

tion number. Thus, one has the sequence δFeO_4 (in $FePO_4$) = 0.300 mm/sec (*22*), δFeO_4Cl = 0.357 mm/sec in $FeMoO_4Cl$, δFeO_4Cl_2 = 0.380 mm/sec in FeOCl,[5] and δFeO_6 = 0.420 mm/sec in $Fe_2(MoO_4)_3$ (*23*).

The limiting ($T \rightarrow 0$°K) value of $H_{internal}$ is 482 kG for $FeMoO_4Cl$ (Table VI). This value is small for a primarily oxygen-ligated ferric system. For instance, $H_{int}(0°K)$ = 524 kG for $Fe_2(MoO_4)_3$ (*23*) and $H_{int}(0°K)$ = 517 kG for $FePO_4$ (*22*). The somewhat lower value may be the result of zero point spin reduction, a feature sometimes evident in both one- and two-dimensional magnets (*24, 25*). The magnitude of the quadrupole splitting is fully consistent with a large electric field gradient generated by the absence of one axial ligand in the square pyramidal (C_{4v}) coordination polyhedra. The valence

[5] Redetermined in our laboratory.

TABLE VI

MÖSSBAUER PARAMETERS[a] FOR $FeMoO_4Cl$ BELOW $T_{Néel}$

T (K)	H (kG)	δ	S_1-S_2	Γ
		(mm sec^{-1})		
1.6	482.0	0.521[b]	1.014	0.37
4.2	482.0	0.521[b]	0.992	0.35
52.9	377.3	0.368	1.067	0.298
56.9	354.9	0.370	1.029	0.312
60.65	323.4	0.370	1.016	0.304
63.25	292.0	0.364	1.02	0.311
65.8	238.6	0.367	1.013	0.385
66.6	217.4	0.365	0.988	0.413
67.07	201.5	0.368	0.963	0.405
67.65	181.0	0.363	0.982	0.432
68.12	157.5	0.364	1.023	0.430

[a] Relative to natural iron, source and absorber at the same temperature.

[b] Source at room temperature.

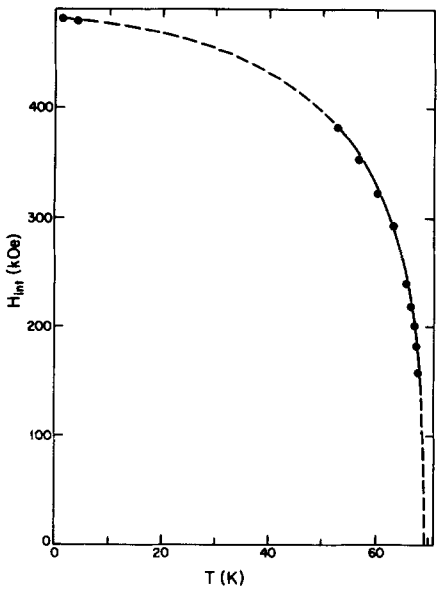

FIG. 8. The internal hyperfine field versus temperature for $FeMoO_4Cl$.

shell occupation contribution to the electric field gradient is expected to be near zero for high spin ferric with its ^6A ground term. The electric field gradient arises primarily from the disposition of the nearest ligand charges. For such an environment and with the relatively "hard base" O^{2-} and "hard acid" Fe^{3+}, one predicts an axially symmetric, *positive*, quadrupole interaction using a point charge model (*26, 27*). That is, the principal component of the electric field gradient tensor (V_{zz}) is positive and the asymmetry parameter $\eta \sim 0$. These observations will be seen important in the succeeding discussion of magnetic structure and are confirmed by single crystal Mössbauer spectra.

As the temperature is decreased, a sharp transition to long range ordering occurs. The temperature dependence of the internal hyperfine field (Fig. 8) indicates $T_{\text{Néel}} = 69.2 \pm 0.1$ K and $H_{\text{int}}(0°\text{K}) = 483$ kG. The slope of the logarithmic plot (Fig. 9) of the reduced hyperfine field (in the vicinity of T_N) is the critical exponent β whose value is 0.3 for the present compound. This is consistent with three-dimensional ordering. A study of the line widths above T_N shows no evidence of slow paramagnetic relaxation.

The more fully resolved, low temperature spectra clearly show the combined effects of magnetic hyperfine splitting with quadrupole perturbation in terms of a shift of the *center* of the inner four Zeeman transitions relative to that of the outer two. The differential shift $(S_1 - S_2)$, where S_1 is the separation of transitions one and two and S_2 is the separation of transitions five and six, is positive and given in Table VI. Its value remains essentially constant near unity and indicates the absence of any "Morin"-type behavior below T_N. For the case of an axially symmetric electric field gradient tensor, the differential shift is related to the quadrupole splitting of the *paramagnetic phase*, ΔE, by the relation: $S_1 - S_2 = -\Delta E(3\cos^2\theta - 1)$ where θ is the angle between the principal component of the electric field gradient tensor, V_{zz}, and the internal hyperfine field (*28*). The foregoing equation has two possible solutions for θ when $S_1 - S_2 \leq \Delta E$, as in the present case. These correspond to $V_{zz} > 0$ and $V_{zz} < 0$. As mentioned previously, V_{zz} is most probably *positive* in view of the known structure and coincidental with the short Fe—Cl bond. The solu-

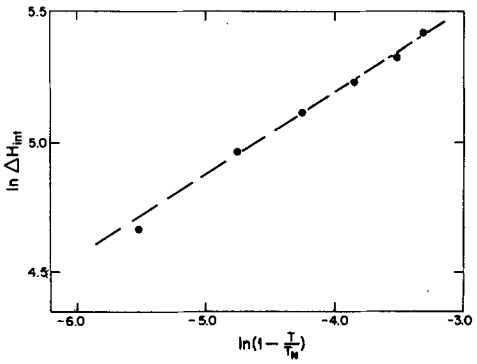

FIG. 9. Logarithmic plot of the reduced hyperfine field in the critical region for $FeMoO_4Cl$.

tion for $V_{zz} > 0$ is $\theta = 90°$. That V_{zz} is in fact positive is confirmed by preliminary single crystal Mössbauer spectra at ~100 K, i.e., $T > T_{Néel}$ such that the direction of γ-ray propagation (E_γ) is along the tetragonal c axis and normal to the $FeMoO_4Cl$ (ab) layers. The angular component of the probability function for $|\frac{1}{2}, \pm\frac{1}{2}> \rightarrow |\frac{3}{2}, \pm\frac{1}{2}>$ (σ γ-ray transitions) is $2 + 3 \sin^2 \theta$ while that for $|\frac{1}{2}, \pm\frac{1}{2}> \rightarrow |\frac{3}{2}, \pm\frac{3}{2}>$ (π γ-ray transition) is $3(1 + \cos^2 \theta)$ where $E_\sigma < E_\pi$ corresponds to $V_{zz} > 0$ and θ is the angle between V_{zz} and E_γ (*28*). Under the foregoing experimental conditions, for a mosaic of single crystals, it was found that the intensity ratio, $I_{\text{low velocity transition}}/I_{\text{high velocity transition}} = 0.45$. This is consistent with V_{zz} parallel to c (i.e., V_{zz} coincides with the Fe—Cl bond vector) and is *positive*. For $T < T_{Néel}$ single crystal spectra with the same orientation, ($E_\gamma \| c$), show a pattern with substantial enhancement of the intensities of the $\Delta M_I = 0$ transitions (transitions 2 and 5) where θ is now the angle between E_γ and H_{int}. The preceeding indicates $\theta \sim 90°$. Under the usual assumption that the magnetization is coincidental with H_{int}, one therefore concludes that *the electron spins and magnetization lie in the $FeMoO_4Cl$ sheets and are essentially normal to the* c *axis*. This result accords with the previous analysis of the combined quadrupole-Zeeman split spectra of the powder. More complete details of zero and high field Mössbauer spectra, very low temperature susceptibility, and magnetization studies of powder and single crystal samples will be published subsequently. Suffice it to say for now that these observations confirm the *two-dimensional magnetic behavior* of the material and that the structural view as chains of corner-sharing *trans*-FeO_4ClCl' octahedra is not tenable.

Aspects of Magnetic Behavior and Structure

That *no* separate and distinct Néel (3D) maximum in χ'_M vs T for $FeMoO_4Cl$ is observed coincidental with its Mössbauer spectra hyperfine splitting (~70 K) is not atypical of 2D-AF systems. The broad lower dimensionality maxima often obscure such 3D maxima and especially for powder measurements. One of the few examples that can be referenced where distinct 3D and 1D maxima are evident in χ'_M vs T for a polycrystalline sample is $(NH_4)_2MnF_5$ (*29*). Separate 3D and lower dimensionality effects are more often discernable as distinct maxima in C_p vs T measurements (*30*). In any event, the primary interlayer interaction leading to the extended 3D ordering of $FeMoO_4Cl$ at ~70 K is undoubtedly the long (3.015 Å) Fe—Cl "contact" discussed in the structure section and that leads to "pseudo" six-coordination of the iron(III). Some supporting evidence for the latter comes from a comparison of the local coordination and isomer shift to those found for chlorobis(pentane - 2,4 - dianato)iron(III), ($Fe(acac)_2Cl$). The reported metal–ligand bond distances and local geometry for the latter are remarkably similar to those for the present system (*18*). Both compounds correspond to FeO_4Cl square pyramids. Similarly, the quadrupole splittings for both are ~1 mm/sec (*31*). However, the isomer shift (relative to iron metal) for $Fe(acac)_2Cl$ is slightly smaller at 0.34 mm/sec in accord with the expected isomer shift systematics for "true" five-coordination[5] (*31*). In other words, the more positive value for Fe MoO_4Cl is consistent with a weak but real chemical interaction. The 3.015-Å contact is the shortest interlayer contact that can be reasonably expected to act as a pathway for superexchange. The possible direct metal–metal interactions between the layers all correspond to distances >5 Å, too large to be significant.

The shortest intralayer Fe—Fe distance is 5.512 Å (see Fig. 1). This is a non-bonded distance that is also far too large for direct exchange interaction. The most viable re-

maining pathway is superexchange through O—Mo—O units that bridge iron atoms along the tetragonal *a* and *b* directions separated by the unit-cell repeat distance, 6.672 Å. The present investigation and other recent work (*32–35*) clearly shows that multi-atom oxo bridge units composed from high symmetry oxyanions such as MoO_4^{2-}, SO_4^{2-}, PO_4^{3-}, AsO_4^{3-} act as rather effective agents for the transfer of magnetic exchange interactions.

The ratio of $T_{Néel}/T_{\chi max}$ for $FeMoO_4Cl$ is 69.2/105 ~ 0.66 implying that the temperature for 3D ordering is some 34% below that representing the two-dimensional effect. Rb_2MnF_4 and K_2MnF_4 show similar (~40%) differentials between $T_{Néel}$ and $T_{\chi max}$, and in this respect $FeMoO_4Cl$ exhibits about the same relative degree of two-dimensionality as the foregoing fluorides. The preceeding differences may be accepted as hallmarks of low dimensionality in that similar differences of $T_{Néel}$ and $T_{\chi max}$ for commonly accepted 3D materials are considerably smaller, generally <10%. It is clear, however, that the interlayer exchange leading to the 3D ordering of $FeMoO_4Cl$ is stronger than that for Rb_2MnF_4 ($T_{Néel}$ = 38.5 K) (*11*), K_2MnF_4 ($T_{Néel}$ = 45.0 K) (*11*), or $[CH_3NH_3]_2MnCl_4$ ($T_{Néel}$ = 47 K, $T_{\chi max}$ = 82 K) (*9*). A two-dimensional *ferric* system to which one might compare the present compound is $CaLaFeO_4$ (*25, 36*). However, both its two- and three-dimensional interactions are considerably stronger, $J/k_B = -38$ K, $T_{Néel}$ = 373 K.

Acknowledgments

The authors thank C. M. Foris for assistance with the X-ray powder diffraction data, Professor C. Dybowski for the ESR spectra, and Mr. M. W. Sweeten for technical assistance. W. M. R. is pleased to acknowledge the support of the National Science Foundation, Division of Materials Research, Solid State Chemistry Program, Grant DMR 8016441.

References

1. L. H. Brixner, H.-Y. Chen, and C. M. Foris, *J. Solid State Chem.* **45,** 80 (1982).
2. L. H. Brixner, H.-Y. Chen, and C. M. Foris, *Mater. Res. Bull.* **12,** 1545 (1982).
3. J. M. Longo and P. Kierkegaard, *Acta Chem. Scand.* **20,** 72 (1966).
4. H. A. Eick and L. Kihlborg, *Acta Chem. Scand.* **20,** 722 (1966).
5. P. Kierkegaard and J. M. Longo, *Acta Chem. Scand.* **24,** 427 (1970).
6. B. Jordan and C. Calvo, *Canad. J. Chem.* **51,** 2621 (1973).
7. L. J. DeJongh, P. Bloembergen, and J. H. P. Colpa, *Physica* **58,** 305 (1972).
8. M. F. Mostafa and R. D. Willet, *Phys. Rev. B* **4,** 2213 (1971).
9. W. D. Van Amstel and L. J. DeJongh, *Solid State Commun.* **11,** 1423 (1972).
10. D. J. Breed, *Phys. Lett.* **23,** 181 (1966).
11. D. J. Breed, *Physica* **37,** 3 (1967).
12. G. K. Wertheim, H. J. Guggenheim, H. J. Levinstein, D. N. E. Buchanan, and R. C. Sherwood, *Phys. Rev.* **173,** 614 (1968).
13. K. G. Srivastava, *Phys. Lett.* **4,** 55 (1963).
14. C. Marcilly and B. Delmon, *C.R. Acad. Sci. Paris Ser. C* **268,** 1795 (1969).
15. C. Cheng and W. M. Reiff, *Inorg. Chem.* **16,** 2097 (1977).
16. R. D. Shannon, *Acta Crystallogr. Sect. A* **32,** 751 (1976).
17. R. L. Martin and A. H. White, *Inorg. Chem.* **6,** 712 (1967).
18. P. F. Lindley and A. W. Smith, *J. Chem. Soc. Chem. Commun.* 1355 (1970).
19. L. Pauling, "The Nature of the Chemical Bond," Cornell Univ. Press, Ithaca, N.Y. (1960).
20. C. C. Torardi, K. Lázár, and W. M. Reiff, to be published.
21. L. J. DeJongh and A. R. Miedema, *Advan. Phys.* **23,** 1 (1974).
22. G. J. Long, A. K. Cheetham, and P. D. Battle, *Inorg. Chem.* **22,** 3012 (1983).
23. P. D. Battle, A. K. Cheetham, G. J. Long, and G. Longworth, *Inorg. Chem.* **21,** 4223 (1982).
24. G. P. Gupta, D. P. E. Dickson, and C. E. Johnson, *J. Phys. C* **13,** 2071 (1980).
25. M. M. N. Guyen-Trut-Dien, M. Vlasse, M. Perrin, and G. Le Flem, *J. Solid State Chem.* **32,** 1 (1980).
26. W. M. Reiff, *Coord. Chem. Rev.* **10,** 37 (1972).
27. G. M. Bancroft, "Mössbauer Spectroscopy, An

Introduction for Inorganic Chemists and Geochemists," McGraw-Hill, New York (1973).
28. N. N. GREENWOOD AND T. C. GIBB, "Mössbauer Spectroscopy," Chapman & Hall, London (1971).
29. S. EMORI, M. INOVE, M. KISHITA, AND M. KUBO, *Inorg. Chem.* **8,** 1385 (1969).
30. F. W. KLAAIJSEN, H. DEN ADEL, Z. DOKOUPIL, AND W. J. HUISKAMP, *Physica B + C (Amsterdam)* **79,** 113 (1975).
31. M. COX, B. F. FITZSIMMONS, A. W. SMITH, L. F. LARKWORTHY, AND K. A. ROGERS, *J. Chem. Soc. Chem. Commun.* 183 (1969).
32. C. NICOLINI AND W. M. REIFF, *J. Solid State Chem.* **44,** 141 (1982).
33. W. M. REIFF AND B. W. DOCKUM, *J. Solid State Chem.* **31,** 407 (1980).
34. C. NICOLINI, G. EISMAN, E. KOSTINER, AND W. M. REIFF, *J. Magn. Magn. Mater.* **15–18,** 1049 (1980).
35. C. NICOLINI AND W. M. REIFF, *J. Phys. Colloq. (Orsay, Fr.)* **C1,** 287 (1980).
36. J. FAVA, M. DONOT, N. T. DINK, A. DAOUDIA, AND G. LEFLEM, *Solid State Commun.* **22,** 833 (1977).